TARGETED OBSERVATIONS OF TROPICAL CYCLONE MOVEMENT BASED ON THE ADJOINT-DERIVED SENSITIVITY STEERING VECTOR

8B.2

Chun-Chieh Wu*, Jan-Huey Chen, Po-Hsiung Lin, and Kun-Hsuan Chou
Department of Atmospheric Sciences, National Taiwan University, Taipei, Taiwan

1. INTRODUCTION

Since 2003, a field program has been conducted under the name of Dropwindsonde Observations for Typhoon Surveillance near the Taiwan Region (DOTSTAR) (Wu et al. 2005). For DOTSTAR, targeted observations constitute one of the most crucial missions. The basis for formulating the observation strategy is to identify the sensitive areas, which would have critical impact on the numerical forecast results and sometimes even the forecast accuracy. Up to the present, three sensitivity products have been used to determine the observation strategy for DOTSTAR. These products are derived from three distinct techniques. First, the Deep-Layer Mean (DLM) winds variance. It is one of the deep-layer steering flows based on the NCEP (National Centers for Environmental Predictions) EFS (Global Ensemble Forecasting System) (Aberson et al. 2003), where areas with the largest forecast deep-layer-mean wind bred vectors represent the sensitive region at the observing time. Second, the Ensemble-Transform Kalman-filter (ETKF, Majumdar 2002). This technique is able to predict the reduction in forecast error variance for feasible deployment of targeted observations based, in this case, on the 40-member NCEP EFS. Third, the Singular Vector (SV) technique (e.g., Palmer et al. 1998). It maximizes the growth of a total energy or kinetic energy norm using, in this case, the forward and adjoint tangent models of the Navy Operational Global Atmospheric Prediction System (NOGAPS, Rosmond 1997; Gelaro et al. 2002).

As mentioned above, the ETKF and SV products are derived from the (total) energy or kinetic energy norm. For the DLM wind variance, high sensitivity has a tendency to appear around the storm region as there is generally higher ensemble variability associated with small displacement of the strong cyclonic wind near the core area. Therefore, none of the above techniques for targeted observations is directly related to the motion (steering flow) of the tropical cyclone.

Theoretical work on the determination of a targeted observation strategy for improving the tropical cyclone track prediction has been lacking in literatures (Rohaly et al. 1998 is a notable exception.). Along with the progress in DOTSTAR, we propose a new method for targeted observations based on the adjoint sensitivity (Zou et al. 1997; Kleist and Morgan 2005) to verify the sensitive areas with respect to the typhoon steering flow. A response function is designed to represent the steering flow at the verifying time, and to assess the adjoint sensitivity with respect to such response functions. A simple parameter is also proposed to interpret the sensitivity with clear physical meanings. The ADSSV will be validated for the binary interaction. The detailed results of this work are also shown in Wu et al. (2006).

2. METHODOLOGY AND EXPERIMENT DESIGN

Adjoint models are powerful tools for many studies that require an estimate of sensitivity of model output with respect to input (Errico 1997). Our study utilizes a component of the MM5 (the fifth generation mesoscale model, Pennsylvania State University/National Center for Atmospheric Research) Adjoint Modeling System (Zou et al. 1997), which was used by Kleist and Morgan (2005) to investigate a snowstorm with a poor forecast. This system includes the nonlinear MM5, its tangent linear model, and corresponding dry-physics adjoint model. The domain for the nonlinear and adjoint models is a 60-km, 85×115 (latitude by longitude) horizontal grid, with 20 sigma levels in the vertical. The initial and boundary conditions are from the NCEP GFS (Global Forecasting System) global analysis (1°×1°) interpolated to the MM5 grids.

* *Corresponding author address:*
Chun-Chieh Wu, Department of Atmospheric Sciences, National Taiwan University, No. 1, Sec. 4, Roosevelt Rd., Taipei 106, Taiwan;
E-mail: cwu@typhoon.as.ntu.edu.tw

Typhoon Mindulle in 2004, one of the observed by DOTSTAR, is chosen as a test case to examine the proposed new method for targeted observations based on the adjoint sensitivity. Note that Mindulle is the sole one out of the ten DOTSTAR cases in 2004 where dropsonde data assimilated into the NCEP GFS model did not improve the track forecasts (figures not shown). The study is based on a 36-h MM5 simulation initialized at 1200 UTC 27 June 2004. The 'forward' and 'backward' integrations were executed by the MM5 forecast model and the adjoint model, respectively, as indicated in Fig. 1. The 'negative' sign before the time indicates the 'backward' integration (using the negative time step) associated with the adjoint model. Figure 2 shows that the model storm moves along (but slightly faster than) the best track from the Central Weather Bureau (CWB) of Taiwan.

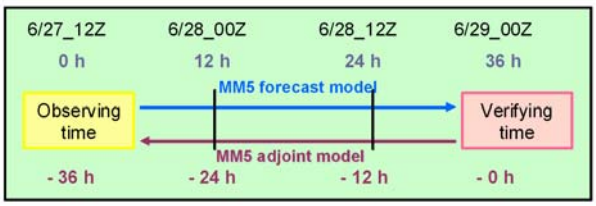

Figure 1. The design of forward and backward model integrations. The 'negative' sign before the time indicates the 'backward' integration (using the negative time step) associated with the adjoint model.

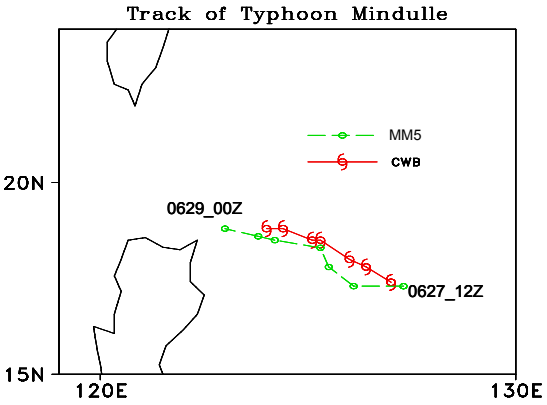

Figure 2. Track of Mindulle from 1200 UTC 27 June to 0000 UTC 29 June from the MM5 forecast and the best-track analysis of CWB.

The work is aimed to identify the sensitive areas at the observing time (1200 UTC 27 June), which will affect the steering flow of Mindulle at the verifying time (0000 UTC 29 June). Therefore, we define the response function(s) as the deep-layer mean wind within the verifying area. A square of 600 km by 600 km, centered around the MM5-simulated storm location (Fig. 3) at the verifying time, is used to calculate the background steering flow (Chan and Gray 1982). Two responses functions are then defined: R_1, the 850-300-hPa deep-layer area average (Wu et al. 2003) of zonal component (u), and R_2, the average of meridional component (v) of the wind vector, i.e.

$$R_1 \equiv \frac{\int_{850hPa}^{300hPa}\int_A u \quad dxdydp}{\int_{850hPa}^{300hPa}\int_A dxdydp}, \text{ and}$$

$$R_2 \equiv \frac{\int_{850hPa}^{300hPa}\int_A v \quad dxdydp}{\int_{850hPa}^{300hPa}\int_A dxdydp}. \qquad (1)$$

In other words, by averaging out the axisymmetric component of the strong cyclonic flow around the storm center, the vector of (R_1, R_2) represents the background steering flow across the storm center at the verifying time. It should be noted that as a wind vector, (R_1, R_2) is totally different from the kinetic energy norm stated above.

In order to interpret the sensitivity with clear physical meanings, we design a unique new parameter, Adjoint-Derived Sensitivity Steering Vector (ADSSV), to identify the sensitive areas at the observing time to the steering flow at the verifying time. The ADSSV with respect to the vorticity field (ς) can be shown as

$$ADSSV \equiv \left(\frac{\partial R_1}{\partial \varsigma}, \frac{\partial R_2}{\partial \varsigma}\right), \qquad (2)$$

where, at a given point, the magnitude of ADSSV indicates the extent of the sensitivity, and the direction of the ADSSV represents the change in the response of the steering flow with respect to a vorticity perturbation placed at that point. For example, if at a given forecast time at one particular grid point the ADSSV vector points to the east, an

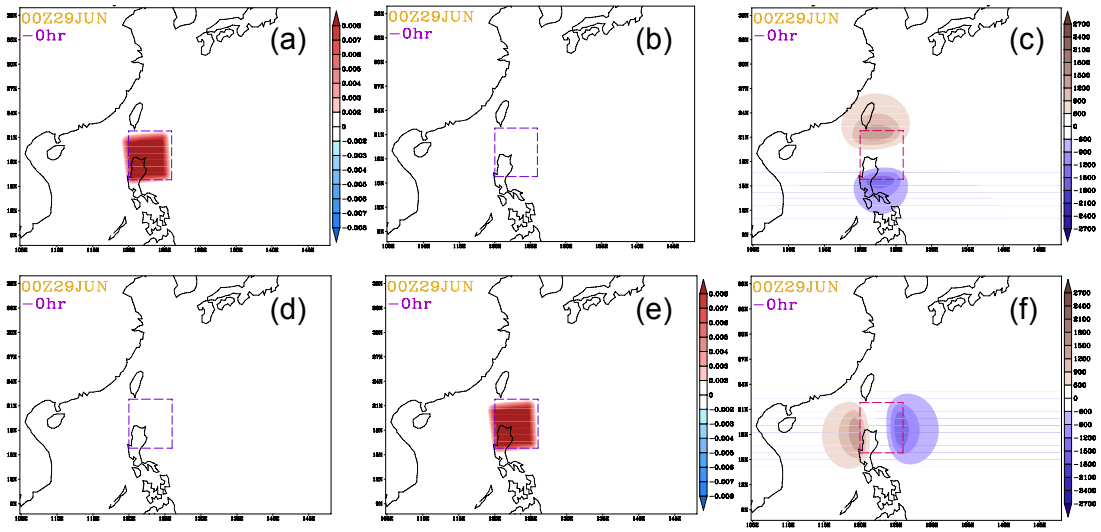

Figure 3. Sensitivity (Gradient) of R1 to (a) u, (b) v, and (c) vorticity, and of R_2 to (d) u, (e) v, and (f) vorticity on the 700 hPa at 0 h. The dashed box represents the verifying area. The magnitude of (c) and (f) is represented in the color bar scale to the right, with the warm (cold) color for positive (negative) value.

increase in the vorticity at the very point at the observing time would be associated with an increase in the eastward steering of the storm at the verifying time.

3. RESULTS

Based on Eq. (1), we first show that the background steering flow (R_1, R_2) at the verifying time in MM5 is (-6.7 m s^{-1}, -0.8 m s^{-1}), which is consistent with the model's westward movement of Mindulle at the verifying time (see Fig. 2 for the modeled storm track). In this paper, only the sensitivity products at 700 hPa are shown. In general, the results of the sensitivity patterns are qualitatively consistent with one another either at 850 or at 500 hPa.

As expected, the sensitivity (i.e., gradient) of R_1 to *u* ($\partial R_1/\partial u$) at -0 h (the initial time of adjoint model) shows a response uniformly distributed over the verifying area (Fig. 3a), while there is no sensitivity of R_1 to *v* ($\partial R_1/\partial v$) (Fig. 3b). To show a general sensitivity to the wind field, we combine the sensitivity of R_1 to *u* and the sensitivity of R_1 to *v* to obtain the sensitivity of R_1 to the vorticity field [$\partial R_1/\partial \varsigma$] (see the derivation in Kleist and Morgan 2005). Again, as expected, a dipolar pattern at -0 h (Fig. 3c) is found, i.e., a positive (negative) vorticity perturbation to the north (south) of the verifying area is associated with a cyclonic (anticyclonic) circulation and thus leads to an increase in R_1 (the zonal component of the mean steering flow). Meanwhile, the sensitivity of R_2 to *u*, *v*, and the vorticity field (Figs. 3d, e, and f) also reveals comparable information. In all, Figs. 3c and 3f can succinctly show the sensitivity of R_1 and R_2 to the flow field with clear physical meanings.

The evolutions of the sensitivity of R_1 and R_2 to the vorticity field are shown in Figs. 4 and 5. The sensitive areas spread from the margin of the verifying area to the outer region as the adjoint model is integrated backward in time. At –36 h (the observing time, 1200 UTC 27 June), the large gradient (and thus the high sensitivity) areas are located in the east and north of the verifying area, and the sensitivity in R_2 is found to be higher than in R_1. This means that vorticity perturbations in those large gradient (sensitive) areas at 1200 UTC 27 June will affect the steering flow of Mindulle at 0000 UTC 29 June, particularly the meridional component of the steering flow.

As shown in Eq. (2), we can combine the result of Figs. 4 and 5 to obtain the evolution of ADSSV with respect to the vorticity field (Fig. 6). Figure 6 clearly shows that the vectors rotate around the

verifying area at -0 h. As the adjoint model integrates backward in time, these vectors evolve and expand outward, with longer vectors (i.e., higher sensitivity) mostly extending at about 800–1300 km from the north to the east of the center of verifying area.

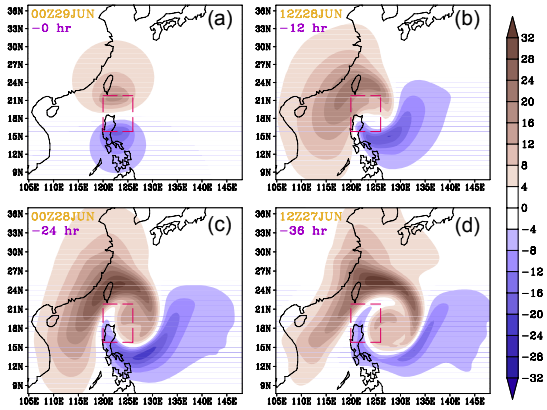

Figure 4. The evolution of sensitivity of R_1 with respect to the vorticity field at 700 hPa (magnitude given by the color bar scale to the right).

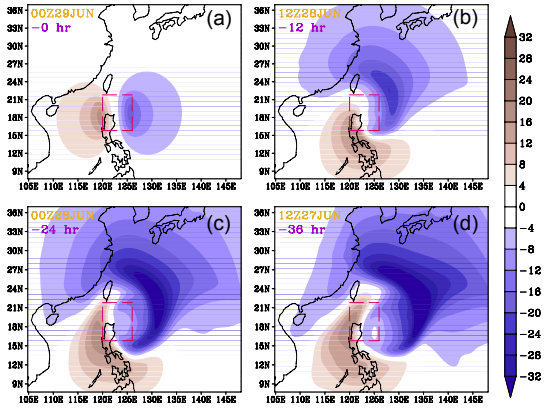

Figure 5. The evolution of sensitivity of R_2 with respect to the vorticity field at 700 hPa (magnitude given by the color bar scale to the right).

In this experiment, we have only demonstrated the ADSSV at one single verifying time. Nevertheless, since the tropical cyclone's final position is affected by the steering flow before and up to the verifying time, it is critical to also calculate the adjoint sensitivity for different verifying times along the storm track; thus the impact of the targeted observations on the entire TC track can be better assessed. Other than performing the 36-h forward model simulation and -36-h backward adjoint integration as shown above, for the same starting (observing) time, we have also conducted the 24-h and 12-h forward and backward integrations to obtain the respective ADSSV associated with the response function (R_1, R_2) based on the respective model-predicted storm location at each verifying time. By combing all the ADSSV at 12, 24, and 36 h as the verifying time in one figure (e.g., Fig. 7), we can clearly identify where the sensitive regions are in affecting the steering flows at 12, 24, and 36 h, respectively, and thus the regions for targeted observations to improve the typhoon track up to the verifying time.

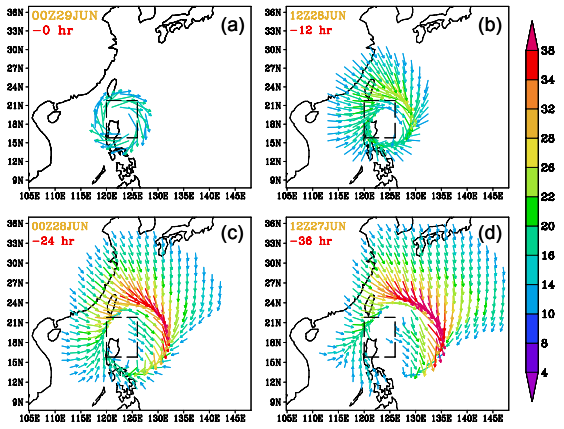

Figure 6. The evolution of ADSSV (magnitude of the vector given by the color bar scale to the right) with respect to the vorticity field at 700 hPa.

To highlight the results, the 12 (in green), 24 (in red) and 36-h (in blue) ADSSV with respect to the vorticity field is plotted in Fig. 7, superposed with the geopotential height field at 700 hPa and the deployed locations of the dropsondes in DOTSTAR. Note that the ADSSV for different verifying times more or less collocates well with one another. Figure 7, in which the vectors in regions of large ADSSV mainly point southward, indicates the southward (northward) component of steering flow strengthens (weakens) with the increase (decrease) in the vorticity in those sensitive areas. Physically, these vectors are located at the edge of the subtropical high, where, if the subtropical high strengthens (i.e., with decreased vorticity), the northward steering increases. The results also show that the extent of the subtropical high is crucial

in determining Mindulle's northward deflection as observed at the verifying time.

Besides the ADSSV with respect to the vorticity field, we also calculate the ADSSV with respect to the divergence field, which is

$$\left(\frac{\partial R_1}{\partial D}, \frac{\partial R_2}{\partial D}\right),$$

where D represents the divergence of the wind field. It is found that the sensitivity to the divergence field (figures not shown) is one order magnitude lower than that to the vorticity field. The above result indicates that the steering flow bears much larger sensitivity to the vorticity field than to the divergence field.

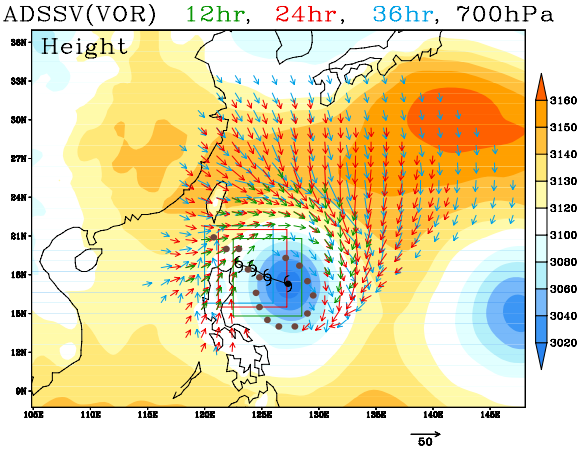

Figure 7. ADSSV with respect to the vorticity field at 700 hPa at 12 (in green), 24 (in red) and 36 h (in blue) as the verifying time, superposed with the geopotential height field (magnitude given by the color bar scale to the right, unit: gpm) at 700 hPa and the deployed locations of the dropsondes in DOTSTAR (brown dots). The 36-h model-predicted track of Mindulle is indicated with the red typhoon symbols for every 12 h.

Note that DOTSTAR's dropsondes are not deployed in the high-sensitivity region in the ADSSV plot in Fig. 7. Meanwhile, the sensitive regions in Fig. 7 are quite different from those indicated by three other independent sensitivity products (figures not shown) currently used for planning the real-time targeted observations for DOTSTAR (Wu et al. 2005). Continued research is needed to assess such differences and to evaluate the strength and weakness of each product (Majumdar et al. 2006; Etherton et al. 2006).

4. A VALIDATION STUDY OF BINARY INTERACTION

In order to validate the sensitivity derived from the adjoint modeling system, we choose Typhoons Fengshen and Fungwong in 2002, which exhibit a clear binary interaction (Yang and Wu 2004). Yang and Wu (2004) investigated this binary interaction from the potential vorticity diagnosis, and they found obvious influence of Fengshen on Fungwong (so-called one-way interaction) during 0000 UTC 23 July to 0000 UTC 25 July (figure not shown).

In this work, the ADSSV is calculated by the MM5 adjoint modeling system. The MM5 forecast model is initialized at 0000 UTC 23 July, with the same domain settings as mentioned above. The forecast location of Fungwong in 48 h is set as the verifying area. The best-track analysis of CWB and the forecast tracks from MM5 are shown in Fig. 8.

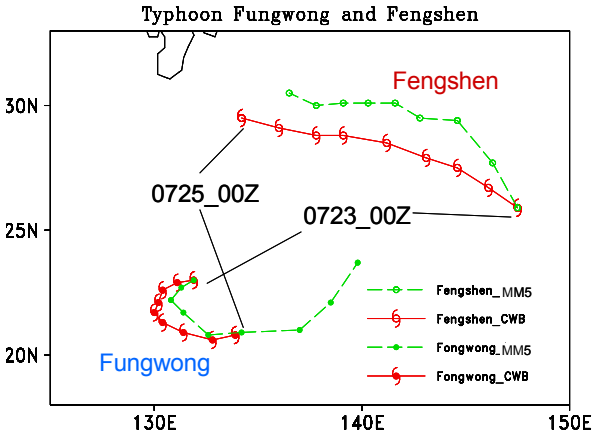

Figure 8. Tracks of Fengshen and Fungwong from 0000 UTC 23 July to 0000 UTC 25 July from the MM5 forecast and the best-track analysis of CWB.

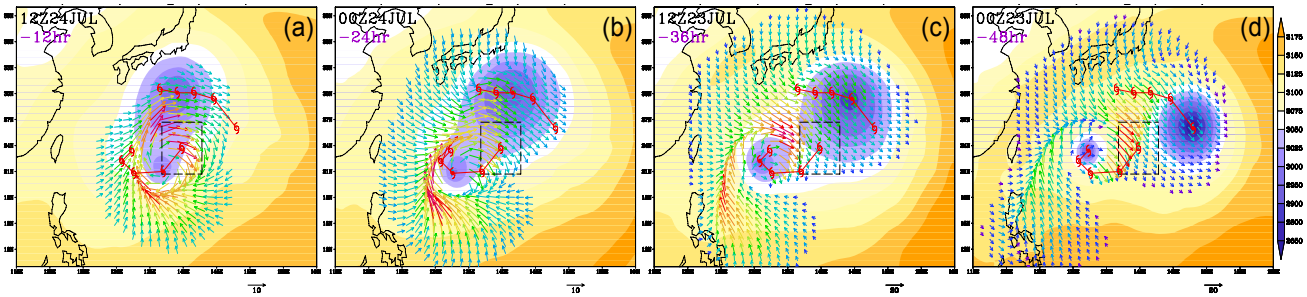

Figure 9. The ADSSV at 700 hPa at (a)-12 (36), (b)-24 (24), (c)-36 (12), and (d)-48 (0) h for 48 h as the verifying time, superposed with the geopotential height field (magnitude given by the color bar scale to the right, unit: gpm) at 700 hPa. The 48 h model-predicted tracks of Typhoon Fungwong and Typhoon Fengshen are indicated with the red typhoon symbols for every 12 h. The box with dash line represents the verifying area which is the location of Typhoon Fungwong.

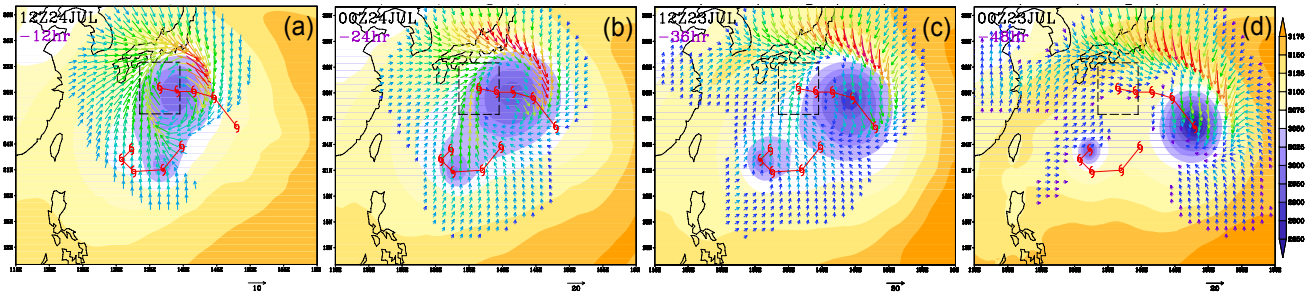

Figure 10. Same as Fig. 9 except the box with dash line represents the verifying area which is the location of Typhoon Fengsheng.

Figure 9 shows the sensitive areas at the different forecast times, that will affect the steering flow of Fungwong at the verifying time. The locations of two typhoons can be recognized by the colors which represent the geopotential height field at 700 hPa in these figures. Following the backward integration, the sensitive areas are always located around Fengshen, and the maximum ADSSV occurs between the two typhoons. It shows that Fengshen is sensitive to the steering flow of Fungwong in the verifying time.

On the other hand, we can set the forecast location of Fengshen in 48 h as the verifying area. It is demonstrated in the ADSSV patterns in Fig. 10 that there is not much sensitivity near Fongwong that would affect the steering flow of Fengshen. Comparison of the ADSSV distribution in Fig. 9d and Fig. 10d apparently shows that Fengshen is sensitive to the steering flow associated with the circulation of Fungwong, but the sensitivity for Fungwong to the steering flow associated with Fengshen is rather insignificant. The maximum ADSSV of Fengshen is mainly located to the north of itself. The above results are consistent with the PV analysis of Yang and Wu (2002), showing the nature of one-way interaction of the two typhoons. Namely, the influence of the circulation associated with the stronger FengShen has an obvious impact on the track of the weaker Fongwong.

5. SUMMARY AND PROSPECTS

In addition to various sensitivity products we have adopted in DOTSTAR, a new sensitivity measurement has been proposed based on the adjoint model. In short, by appropriately defining the response functions to represent the mean steering flow at the verifying time, we can derive its sensitivity to the flow field at the observing time to help formulate the observation strategy. In particular, a simple vector, the ADSSV with respect

to the vorticity field, is proposed to clearly demonstrate the sensitivity to the storm motion. We believe that ADSSV can be applied to scientific research in many aspects and can be tested in the field project to help improve the typhoon track prediction.

Subsequent work is being carried out to consolidate this study, and will be presented in other papers.

(1) Linearity test and impact of the dry-physics adjoint model

The adjoint model is designed based on TLM, which is a linear assumptive model. As already demonstrated in Kleist and Morgan (2005), in order to validate this assumption, perturbations that evolve linearly via the TLM need to be compared with difference fields obtained from two nonlinear model forecasts to show the validity of the linear assumption.

Note that the adjoint model employed here does not include the moist physics. Although it is definitely critical to the development of the tropical cyclone system, we believe that the tropical cyclone movement is mainly controlled by the large-scale flow field, which is less likely to depend on the moist physics. Further test on this can be conducted using the moist version of the adjoint model.

(2) Impact study

The above validation study of the binary interaction between Fengshen and Fongwong indicates that the ADSSV can well represent the signal of the one-way binary interaction process. Besides the binary interaction, the ADSSV can also be used to show how the critical weather system affects the typhoon motion, such as the impact from the approaching trough. To validate the sensitivity derived from the adjoint modeling system in more details, we also plan to design other experiments, such as to perturb the wind (vorticity) fields in the initial time (such as those in the area with large magnitude of ADSSV), and investigate the response to the simulated typhoon track.

(3) Application of the ADSSV method to other adjoint modeling systems

Besides the MM5 adjoint modeling system, there are other adjoint models, such as NOGAPS. How the ADSSV method will appear in different modeling systems is an interesting issue worthy of further study.

(4) Operation in the field program

While the above task continues, we are in the process of implementing the currently designed method (using ADSSV) for real-time use in DOTSTAR, as well as for Atlantic hurricanes (in collaboration with Sim Aberson), in 2005 (Etherton et al. 2006). A longer model integration time would then be called for because the DOTSTAR operation would require a lead time of at least 48 h. The preliminary test is showing consistent results when we run the model for up to 84 h, thus indicating the feasibility of the current system used in the DOTSTAR operation. We believe that using the method of ADSSV in DOTSTAR will shed new light on the targeted observations for tropical cyclones.

Acknowledgments. The work is supported through the National Science Council of Taiwan by Grants NSC92-2119-M-002-009-AP1 and NSC93-2119-M-002-013-AP1 and the Office of Naval Research Grant N00014-05-1-0672. The authors wish to thank Sim Aberson, Frank Marks, Sharan Majumdar, Michael Morgan, Melinda Peng and Carolyn Reynolds for their helpful suggestions and research collaborations.

References

Aberson, S. D., 2003: Targeted observations to improve operational tropical cyclone track forecast guidance. *Mon. Wea. Rev.*, **131**, 1613–1628.

Chan, J. C.-L., and W. M. Gray, 1982: Tropical cyclone movement and surrounding flow relationship. *Mon. Wea. Rev*., **110**, 1354-1376.

Errico, R. M., 1997: What is an adjoint model? *Bulletin of Amer. Meteor. Soc.*, **78**, 2577–2591.

Etherton, B., C.-C. Wu, S. J. Majumdar, and S. D. Aberson, 2006: Comparison of the targeted observation strategies for Atlantic hurricanes in

2005. Preprint, 27th Conf. on Hurricanes and Tropical Meteorology, Amer. Meteor. Soc.

Gelaro, R., T. E. Rosmond, and R. Daley, 2002: Singular vector calculations with an analysis error variance metric. *Mon. Wea. Rev.*, **130**, 1166-1186.

Kleist, D. T., and M. C. Morgan, 2005: Interpretation of the structure and evolution of adjoint-derived forecast sensitivity gradients, *Mon. Wea. Rev.*, **133**, 466–484.

Majumdar, S. J., C. H. Bishop, R. Buizza and R. Gelaro, 2002: A comparison of ensemble-transform Kalman-filter targeting guidance with ECMWF and NRL total-energy singular-vector guidance, *Q. J. R. Meteorol. Soc.*, **128**, 2527–2549.

Majumdar, S. J., S. D. Aberson, C. H. Bishop, R. Buizza, M. S. Peng and C. A. Reynolds, 2006: A comparison of adaptive observing guidance for Atlantic tropical cyclones. Submitted to *Mon. Wea. Rev.*

Palmer, T. N., R. Gelaro, J. Barkmeijer, and R. Buizza, 1998: Singular vectors, metrics, and adaptive observations. *J. Atmos. Sci*., **55**, 633–653.

Rohaly, G. D., R. H. Langland, and R. Gelaro, 1998: Identifying regions where the forecast of tropical cyclone tracks is most sensitive to initial condition uncertainty using adjoint methods. Preprints, 12th Conf. on Numerical Weather Prediction, Phoenix, Arizona, Amer. Meteor. Soc., 337-340.

Rosmond, T. E., 1997: A technical description of the NRL adjoint model system, NRL/MR/7532/97/7230, Naval Research Laboratory, Monterey, Calif., 93943-5502, 62pp.

Wu, C.-C., T.-S. Huang, W.-P. Huang, and K.-H. Chou, 2003: A new look at the binary interaction: Potential vorticity diagnosis of the unusual southward movement of Typhoon Bopha (2000) and its interaction with Typhoon Saomai (2000). *Mon. Wea. Rev.*, **131**, 1289-1300.

_____, P.-H. Lin, S. D. Aberson, T.-C. Yeh, W.-P. Huang, J.-S. Hong, G..-C. Lu, K.-C. Hsu, I-I Lin, K.-H. Chou, P.-L. Lin, and C.-H. Liu, 2005: Dropwindsonde Observations for Typhoon Surveillance near the Taiwan Region (DOTSTAR): An Overview. *Bulletin of Amer. Meteor. Soc.*, **86**, 787-790.

_____, J.-H. Chen, P.-H. Lin, and K.-H. Chou, 2006: Targeted observations of tropical cyclone movement based on the adjoint-derived sensitivity steering vector. Submitted to *J. Atmos. Sci.*

Yang, C.-C., and C.-C. Wu, 2004: Binary interaction between Typhoons Fengshen (2002) and Fungwong (2002) based on the potential vorticity diagnosis. 26th Conf. on Hurricanes and Tropical Meteorology, *Amer. Meteor. Soc.*, Boston, MA. 663-664

Zou, X., F. Vandenberghe, M. Pondeca, and Y.-H Kuo, 1997: Introduction to adjoint techniques and the MM5 adjoint modeling system. NCAR Technical Note, NCAR/TN-435+STR, 110pp. [Available from NCAR, P.O. Box 3000, Boulder, CO 80307-3000.].